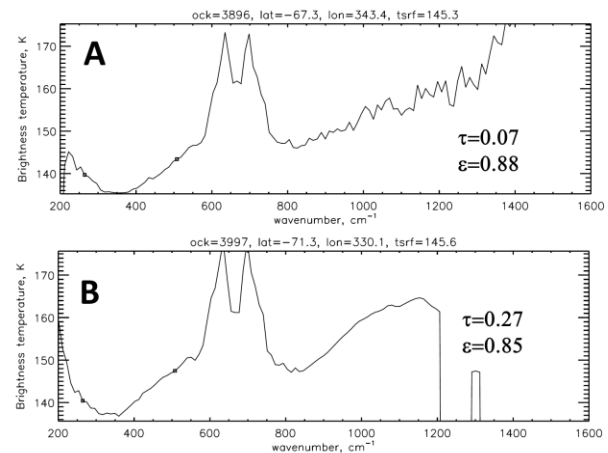


**EVOLUTION OF THE MARTIAN SOUTHERN SEASONAL POLAR CAP EMISSIVITY DURING SPRING OF MY24-26.** A. Pankine<sup>1</sup>, <sup>1</sup>Space Science Institute, 4765 Walnut St, Suite B, Boulder, CO 80301 (apankine@spacescience.org).

**Introduction:** Seasonal Polar Caps (SPC) form on Mars from condensing atmospheric CO<sub>2</sub> each winter and recede during spring. A small patch of CO<sub>2</sub> ice dubbed Southern Polar Residual Cap (SPRC) is present year-round near the south pole. The temperature of the surface CO<sub>2</sub> ice in equilibrium with atmosphere is maintained near 140 K. Early observations from orbiting spacecraft revealed brightness temperatures significantly below the equilibrium temperature over portions of the SPC [1]. Later analysis [2, 3] suggested that this ‘cold spots’ are due to low surface emissivity associated with the presence of fine-grained CO<sub>2</sub> ice on the ground. This work presents the first systematic retrievals of SPC surface emissivity during southern spring (Ls=180–270°) using data collected by Mars Global Surveyor (MGS) Thermal Emission Spectrometer (TES) [4] in Mars Years (MY) 24, 25 and 26. Evolution of the SPC in the Southern Polar region (SPR) was analyzed in [5] using TES data from the pre-mapping aero-braking phase of the mission (MY23 Ls=180–360° MY24 Ls=0–24°). This work expands this analysis to data collected during the mapping phase of the mission and uses a different retrieval approach. MY24 and MY26 were ‘typical’ Mars year with relatively low dust opacities over southern SPC during spring, while in MY25 a Global Dust Storm (GDS) developed in the early spring (at Ls~185°) significantly increasing dust opacities over SPC until late spring.

**Retrieval methodology:** Retrievals of surface emissivity and atmospheric dust opacity over Martian SPCs is a difficult problem. Low surface and atmospheric temperatures result in a low thermal contrast between atmosphere and surface, and a weak spectral signal for surface emissivity and atmospheric dust (see Figure 1 for examples of TES spectra over southern SPC). In addition, TES spectra of cold targets are significantly affected by a radiometric error at wavenumbers larger than ~800 cm<sup>-1</sup>, which produces an upward slope or very low radiances at this spectral range [6]. To alleviate these problems, the dust opacity  $\tau$  and surface emissivity  $\epsilon$  are retrieved using TES radiances observed at wavenumbers 264 cm<sup>-1</sup> and 508 cm<sup>-1</sup> (corresponding to wavelengths of ~40  $\mu$ m and ~20  $\mu$ m, respectively). At these wavenumbers the dust extinction differs by a factor of ~2, while the CO<sub>2</sub> frost emissivity is similar for a wide range of ice grain sizes [5]. This allows distinguishing the effects of atmospheric

dust from surface effects in the TES spectra. The surface temperature was fixed to the condensation temperature of the CO<sub>2</sub> ice over the SPC. To improve the quality of the data, 10 consecutive spectra were averaged. To improve retrieval accuracy, only the data collected between local times of 8 am and 8 pm, and only when the sun is above the horizon, were used in the retrieval. Figure 1 shows examples of TES spectra and retrievals over southern SPC in MY24.



**Figure 1. Examples of TES MY24 spectra and retrievals, with retrieved dust opacity values  $\tau$  and CO<sub>2</sub> frost emissivity  $\epsilon$  shown on the plots. A) Spectrum over SPC, low dust opacity, low CO<sub>2</sub> frost emissivity. B) Spectrum over SPC, high dust opacity, low CO<sub>2</sub> frost emissivity.**

**Results:** Figure 2 shows polar maps of retrieved thermal reflectance ( $1-\epsilon$ ) at 20  $\mu$ m at selected time periods during southern hemisphere spring (results for atmospheric dust retrieval will be presented elsewhere). CO<sub>2</sub> emissivity varies across the SPC and with time. At the beginning of spring high reflectance (low emissivity) areas are found near the outer edge of the SPC between longitudes 225°–360°–45° E. After Ls~245° high reflectance area occupies most of the area of the receding SPC. The spatial and temporal evolution of CO<sub>2</sub> emissivity is remarkably similar in the observed years (MY24–MY26) and also consistent with the evolution observed in MY23 [5]. The areas of high reflectance (low emissivity) were previously interpreted [2,3,5] as areas with small CO<sub>2</sub> ice grains. From comparison with emissivity estimates based on Mie modeling [7] the CO<sub>2</sub> particles in these areas have sizes between 1 mm and 1 cm with possible admixture of H<sub>2</sub>O

ice and/or dust. The areas of high emissivity are interpreted as CO<sub>2</sub> grains larger than 1 cm and slab ice.

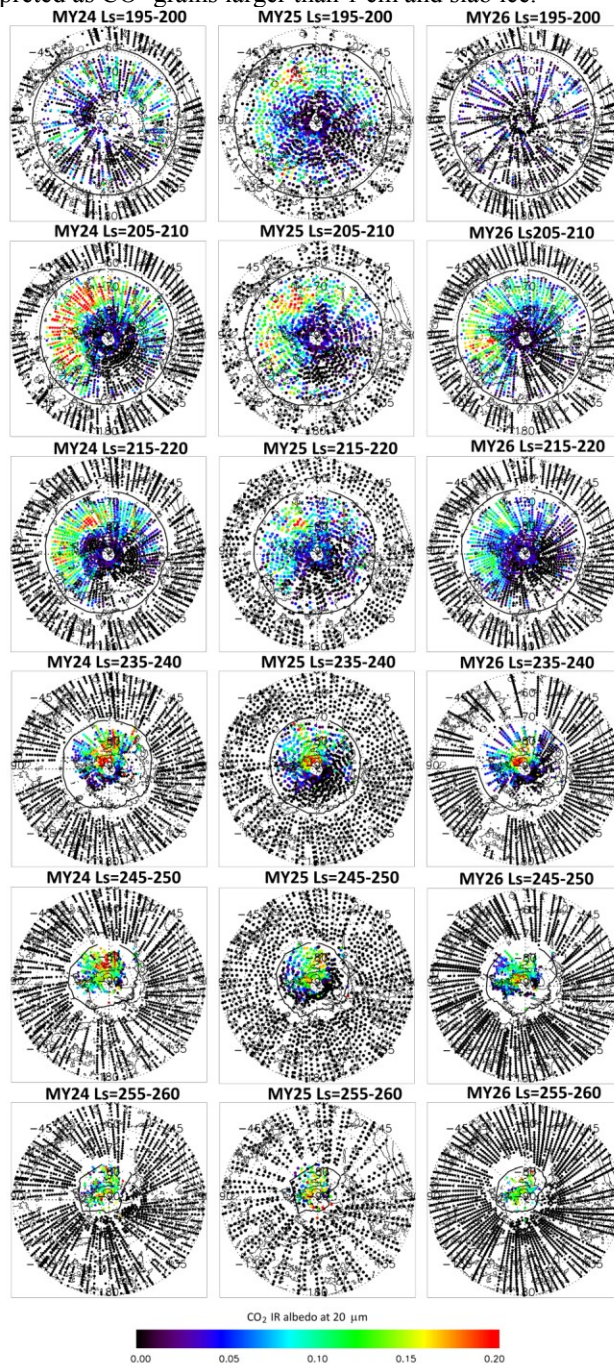


**Figure 2.** Polar maps of retrieved surface thermal reflectance ( $1-\epsilon$ ) at 20  $\mu\text{m}$  in the SPR for Ls=195-260° in MY24–26. Outer edge of the map is at latitude -50°. East longitudes increase clockwise from top. Light contours are MOLA topography, heavy contour is approximate edge of the SPC.

The peculiar asymmetry in distribution of CO<sub>2</sub> grain sizes across SPC was previously interpreted as being due to two different deposition regimes arising

from atmospheric circulation modified at the SPR by the large-scale topography of the Hellas impact basin (centered on 25° S and 65° E, upper right on maps in Figure 2) [8]. Over areas west of the Hellas, where low CO<sub>2</sub> emissivity areas are found, atmospheric precipitation dominates over surface deposition, forming smaller grains. East of the Hellas frost is accumulated by direct deposition, forming larger grains and dark CO<sub>2</sub> slab ice.

**References:**

[1] Kieffer, H. H. et al. (1976) *Science*, 194, 1341–1344. [2] Forget, F. et al. (1995) *J. Geophys. Res.*, 100, 21219–21234. [3] Titus, T. et al. (2001) *J. Geophys. Res.*, 106, 23181–23196. [4] Christensen, P. R. et al. (2001) *J. Geophys. Res.*, 106, 23823–23871. [5] Kieffer, H. H. et al. (2000) *J. Geophys. Res.*, 105, 9653–9699. [6] Pankine, A. A. (2015) *Planet. Space Sci.*, 109, 64–75. [7] Titus, T. N. et al. (2008) *The Martian Surface: Composition, Mineralogy, and Physical Properties*, 578–598. [8] Colaprete, A. et al. (2005) *Nature*, 435, 184–188.